Volume 5, No. 6; December 2017

Advances in Image And Video Processing

ISSN: 2054-7412

Society for Science and Education - United Kingdom

TABLE OF CONTENTS

EDITORIAL ADVISORY BOARD

DISCLAIMER

All the contributions are published in good faith and intentions to promote and encourage research activities around the globe. The contributions are property of their respective authors/owners and the journal is not responsible for any content that hurts someone's views or feelings etc.

AIVP ADVANCES IN IMAGE AND VIDEO PROCESSING
SOCIETY FOR SCIENCE AND EDUCATION UNITED KINGDOM
VOLUME 5, ISSUE 6
ISSN 2054-7412

Real-Time Noise Classification of Medical Image via Online Machine Learning Algorithm

[1]Yuchou Chang
[1]Computer Science and Engineering Technology Department, University of Houston - Downtown, Houston, United States
changy@uhd.edu

ABSTRACT

Medical image is generally deteriorated by noise due to signal acquisition, signal processing, and other reasons. Noise classification of medical image is able to enhance post-processing tasks like medical image segmentation, registration, and analysis. Due to real-time requirements of medical image analysis for clinical applications, noise classification of medical image is desired to be fast for meeting real-time requirements. On the other hand, online learning algorithms have been studied for processing online data in real-time mode, which can produce rapid learning model based on adjustments of new incoming data. In this paper, we investigate perceptron algorithm - a classical online learning method for noise classification in parallel magnetic resonance imaging (pMRI). Noise generated in pMRI is quickly classified and online classification model is updated in real-time simultaneously. Experimental results demonstrate that noise and brain tissues existing MR images is able to be classified dynamically with the perceptron algorithm.

Keywords: Noise Classification, Online Learning Algorithm, Medical Image, Noise Distribution, and Parallel Magnetic Resonance Imaging.

1 Introduction

Image acquisition and processing is generally accompanied by noise, which is generated in the final image with various reasons during imaging stages. Noise can deteriorate image quality. There are two types of causes that generate noise: external causes and internal causes. Each type of noise is composed of several sources of noise. For example, external noise refers to the noise caused by the external interference of the system by the electromagnetic wave or the power source entering the system. This type of noise may be Gaussian noise, impulse noise and other noise synthesis cumulative. Identification and classification of medical image noise level is important for other tasks like image denoising [1-3], object recognition [4-6], and motion tracking [7-9]. On the other hand, real-time is another requirement in many image-based applications like medical image guided intervention or surgery [10]. In the field of medical image acquisition and processing, due to imperfection of imaging system, transmission media and recording equipment, medical images are often contaminated by various noises during the formation and transmission of medical images. Noise is not related to the object of study as useless information, which disturbs the observability of the image. Therefore, the classification and identification of noise is important in medical image processing. If the image noise is not suppressed, it will be difficult to process the image directly, which may even lead physicians to make incorrect judgments when patient's condition is diagnosed.

DOI: 10.14738/aivp.56.4084
Publication Date: 31st December, 2017
URL: http://dx.doi.org/10.14738/aivp.56.4084

Online learning [11, 12] is a commonly used machine learning algorithm in the industry and can work well in many scenarios. Online Learning can make real-time and rapid learning model adjustments based on online feedback data so that the learning model can reflect online changes timely and improve the accuracy of online prediction. The process of online learning includes presenting the learning model's predictions to the user, collecting user feedback data, and then training the learning model to form a closed-loop system. The ideal algorithm is to be able to get a good learning model with a small amount of data. Online learning uses only current and past data and the future is unknown. Therefore, for online learning, it pursues the best strategy that can be designed with all the data dynamically. The difference with this optimal strategy is called regret: regret doesn't choose the optimal strategy rightly from the beginning. With more data over time, the difference will become smaller. Because any assumptions about the data is not made, the optimal strategy may be not perfect (for example, classifying all data correctly).

In magnetic resonance imaging (MRI), the technique of sensitivity encoding (SENSE) [13] uses a phased array coil with different sensitivities to place the target around. In order to maintain the spatial resolution unchanged, sampling rate in *k*-space is decreased to reduce the number of phase-encoding sampling steps, so that the imaging speed is accelerated. As a parallel MRI technique, SENSE requires to use the coil sensitivity profile unfolding aliasing image, and the coil sensitivity map is pre-scanned. Parallel MRI techniques lead to a significant reduction in signal-to-noise ratio. For example, if reduction factor R = 2, the image SNR decreases by $\sqrt{2}$, which is around 40%. This disadvantage is usually not only a problem in high fields (where higher signal-to-noise ratios are higher) and but also in certain anatomical areas (e.g. relatively symmetrical and uniform brains). Such reconstruction errors increase as the acceleration factor (R) increases.

In order to characterize noise distribution in SENSE reconstruction based MR image, an online learning framework is proposed in the paper. Online learning is applied to classify and identify noise distribution in real-time mode of reconstructed MR images. The paper is organized as follows. The first section introduces context of the proposed research work. The second part presents the background of the relevant methods. The third one gives the proposed method of the real-time noise classification of MR images. Experimental results and conclusion will be provided in the fourth and fifth sections, respectively.

2 Background

In traditional machine learning method, after the learning model is trained, the update cycle of the learning model will be longer since training dataset cannot be updated quickly. Therefore, after the model is online, it is generally static (it will not change for a period of time). Any interaction with the online learning model (assuming if the prediction is wrong) can only be corrected at the next stage of the model update. Online learning algorithms are able to adjust the learning model dynamically based on the results of online prediction. If wrong prediction or classification is produced by the learning model, it will be corrected in time. Therefore, online learning can reflect online changes in a real-time manner. Online Learning can make real-time and rapid learning model adjustments based on online feedback data, so that the learning model can timely reflect online changes and improve the accuracy of online prediction. The optimization goal of Online Learning is to minimize the total loss function.

As shown in the Figure 1, a closed-loop system of online learning contains several steps. At time t, learning model receives data x_t, learning model provides a prediction or classification strategey h_t, and environment will give the correct answer y_t. Learning model will have a loss $l(h_t, y_t)$ at the moment.

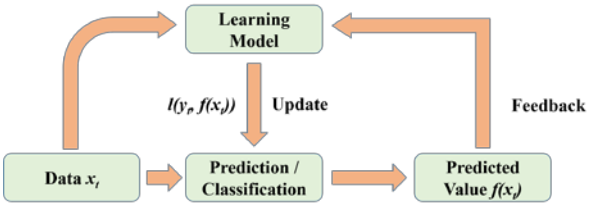

Figure 1. Framework of online learning algorithm.

Learning model learns domain knowledge when learning model receives data each time. The repeated steps of online learning is as follows: (1) receiving data x_t, (2) learning model selects a strategy h_t and make a prediction $h_t(x_t)$, and (4) repeat the above steps to produce loss each time. In order to evaluate learning quality each time, the concept of regret is defined as

$$R(T) = \sum_{t=1}^{T} l_t(h_t) - min \sum_{t=1}^{T} l_t(h), h \in \mathcal{H} \quad (1)$$

, where h is the optimal strategy of learning model is to make a good $h_t = f(x_t)$ each time to make R(T) minimum. The optimal strategy is to fix h, but if we can choose a good h_t to adapt to the learning problem (x_t, y_t) every time, the total loss may be smaller. But this is difficult. since a good strategy h_t has to be set and correct answer y_t should be known. If the learning problem is very different from the previous one and the answer is difficult to be obtained. For the optimal strategy, if all the learning problems and answers are known in advance, so optimal strategy is more likely to have a minimum total loss. Therefore, the average regretR (T) / T is considered since it is smaller with T becomes smaller. If an online algorithm is not no-regret, it means:

$$\lim_{n \to \infty} \frac{R(T)}{T} \to 0 \quad (2)$$

On the other hand, a parallel MRI technique is used to apply online learning algorithm for identifying noise distribution. MR images can be generated by fast parallel MR imaging to speed up imaging. SENSE technology is one of the widely used parallel MR image reconstruction techniques. SENSE's rapid performance makes patients more comfortable and reduces clinical costs. Although more noise and aliasing artifacts are produced as a compromise of imaging acceleration in the SENSE method, it has been widely used in clinical applications. Acronyms [14] of SENSE implementation on five MR scanner vendors are shown in the Table 1. The general SENSE equation is

$$Ef = d \quad (3)$$

, where d is a vector formed from k-space data on all channels, f is the complete FOV image to be solved, and E is the sensitivity encoding matrix. Using an unwrapping operation, the signal is separated for each pixel in a reduced FOV to produce a unaliased, full field image. In addition, geometric factors, a priori signal-to-noise ratio (SNR) estimates, and important criteria for designing a coil array consist of

$$g(\rho) = \sqrt{[(S^{H}\Psi^{-1}S)^{-1}]_{\rho,\rho}\,(S^{H}\Psi^{-1}S)_{\rho,\rho}} \quad (4)$$

where ρ is pixel, S is the sensitivity matrix, and Ψ is the receiver noise covariance matrix. During parallel MR imaging, geometry related noise enhancement increases rapidly when reduction factor increases. The proposed method identifies the distribution of noise and aliasing artifacts by using geometric factors to identify enhanced edge detection of MR brain images.

Table 1 shows acronyms of sensitivity encoding (SENSE) implementation on five MR scanner vendors.

MR Scanner Vendors	Acronyms of SENSE Implementation
Siemens	mSENSE
General Electric (GE)	ASSET
Philips	SENSE
Hitachi	RAPID
Toshiba	SPEEDER

3 Proposed Method

Perceptron [15, 16] is a supervised linear online classification algorithm. The algorithm divides the input examples into positive and negative ones. After learning the results, the algorithm estimates *w* from the examples in the training data. The algorithm then predicts the category of input data based on the sign of the product of the feature vector *x* and the parameter vector *w*. The perceptron algorithm accepts an input instance *x* and determines its category based on the weight vector *w*. Let input *x* be a d-dimensional real vector, *w* is the weight vector of the model, and it is also a d-dimensional real vector. The binary perceptron divides the input *x* into two categories according to the output function $w^T x$. It divides instance *x* of $w^T x > 0$ into positive ones. On the other hand, it divides *x* into negative ones when $w^T x < 0$. Given training data, what the perceptron algorithm learns is the model's weight vector *w*. Initialization weight vector *w* is 0. In iteratively determining the positive and negative cases of error, when positive examples are negative, $w(t+1) \leftarrow w(t) + x$, and when negative examples are positive, $w(t+1) \leftarrow w(t) - x$.

MRI noise [17] can worsen medical image analysis performance because many image analysis algorithms like segmentation and registration are sensitive to noise within the image. Noise also reduces the anatomy boundary accuracy in MR images. Noise generation in MR scans is complicated. It is related to electricity current, coil configuration, and magnetic fields. Noise should be suppressed in MR image. Suppose the input space (pixel values in MR image) is X and the output space is Y = {-1, +1}. Each feature vector x∈X of the instance is corresponding to each point in the input space. The output y∈Y represents the class (pixel's noise level) of the example. The function from input space to output space is

$$p(x) = sign(w \cdot x + b) \tag{5}$$

, where *p* is called perceptron, *w* represent weight vector, and *b* is bias. The $w \cdot x$ denotes the inner product of *w* and *x*,

$$\sum_{i=1}^{n} w_i x_i = w_1 x_1 + w_2 x_2 + \cdots + w_n x_n \tag{6}$$

, where *sign* is sign function. It is

$$p(x) = \begin{cases} +1, & if\ x >= 0 \\ -1, & else \end{cases} \tag{7}$$

Sensitivity encoding (SENSE) is a typical image-based MRI reconstruction method. It is non-aliased in the image domain. After inverse Fourier transform of *k*-space data, SENSE reconstructs the aliased coil images. During the inverse Fourier transform, the field of view (FOV) is reduced by 1 / R (R is a reduction factor for undersampled *k*-space). The same information is contained in the smaller area, which leads to folded aliasing artifacts. According to the Eq. (1), the brain MR image is reconstructed by SENSE algorithm as shown in Figure 2 (d). It can be seen that the reconstructed image deteriorates due to noise and aliasing artifacts as a tradeoff of acceleration of the undersampled signal in *k*-space.

In addition, the geometry factor aligning with noise distribution is generated as shown in Figure 2 (e). It can characterize the distribution of noise and aliasing artifacts appearing in the SENSE image in Figure 2 (d). The higher value of the geometric factor represents the lower SNR of the corresponding pixel location in the image. The geometric factor is able to guide the noise distribution and intensity in the reconstructed SENSE image. The proposed method uses geometric factor values to represent noise levels in the MR image domain. Noise and true pixel values should be classified into different classes for identifying noise. The value of $p(x)$ (+1 or -1) is used to classify whether MR image pixel x is true value (+1) or noise (-1). Perception machine is a linear classification model. All need to do is find an optimal w and b value that satisfies the separating hyperplane $w \cdot x + b = 0$.

The purpose of the perceptron learning is to find a separation hyperplane that completely separates the true value pixels and noise instances of the training set. Since a pixel with higher geometry factor value represents higher level of noise, the neighbor pixels also have a high probability to be noisy pixels. For this reason, neighbor 8 pixels of the local 3 x 3 window are extracted and combined with the center pixel as a feature vector representing the local window noise level. To find such a hyperplane, the perceptron model parameters w and b are determined through minimizing the loss function. For the choice of loss function, distance from the misclassified point to the hyperplane is calculated as

$$\frac{1}{||w||}|w \cdot x_0 + b| \tag{8}$$

, where $||w||$ is L2 norm. For a misclassified pixel (x_i, y_i), it has $-y_i(w \cdot x + b) > 0$. The distance between this misclassified pixel and hyperplane is calculated as

$$-\frac{1}{||w||} y_i(w \cdot x_0 + b) \tag{9}$$

Therefore, the loss function of all misclassified pixels to the hyperplane is defined as

$$L(w, b) = -\sum_{x_i \in M} y_i(w \cdot x_0 + b) \tag{10}$$

, where M is the set of all misclassified pixels in MR image. If there is no misclassified pixels, the loss function is zero. If there are fewer misclassified pixels and they are closer to the hyperplane, the loss function is also smaller. Perceptron learning algorithm is driven by misclassified pixels, so we use stochastic gradient descent method to alternatively solve the following minimization problem.

$$min_{w,b} L(w, b) = -\sum_{x_i \in M} y_i(w \cdot x_0 + b) \tag{11}$$

In this way, it can be expected through iteration that the loss function $L(w, b)$ value continues to decrease until it reaches zero.

4 Experimental Results

As shown in Figure 2 (a), the reference image 1 has little noise and aliasing artifacts. It is completely sampled but requires longer MR scanner acquisition time. Figure 2 (b) and (c) show a coil image and its coil sensitivity profile. Coil sensitivity creates noise and aliasing artifacts in the reconstructed MR image as shown in Figure 2 (d), thereby reducing image quality. It can be seen that noise exists in white matter, gray matter, and cerebrospinal fluid (CSF) of brain image. The corresponding geometric factor map as shown in Figure 2 (e) indicates the distribution of noise and aliasing artifacts. The g-factor is generally greater than 1, and the higher value of g-factor represents higher level of noise. For this reason, we set threshold of g-factor with different values to test the perceptron online learning algorithm. As indicated in the Table 2, 3 thresholds (1.0, 1.5, and 2.0) are list for performance comparison of the perceptron algorithm. Different thresholds represent different levels of noise. The

higher value means only very noisy pixels are considered as noise in the image and the tolerance of noise is also higher. For the g-factor map, if a pixel value is greater than threshold, it is considered as the noisy pixel. Otherwise, it is considered as a pixel with true value under acceptable noise level. In addition, the reference MR brain image 2 is shown in Figure 3 (a). It is completely sampled but requires longer MR scanner acquisition time. Figure 3 (b) and (c) show a coil image and its coil sensitivity map. Coil sensitivity creates noise and aliasing artifacts in the reconstructed MR image as shown in Figure 3 (d). The corresponding geometric factor map as shown in Figure 3 (e) indicates the distribution of noise and aliasing artifacts in Figure 3 (d).

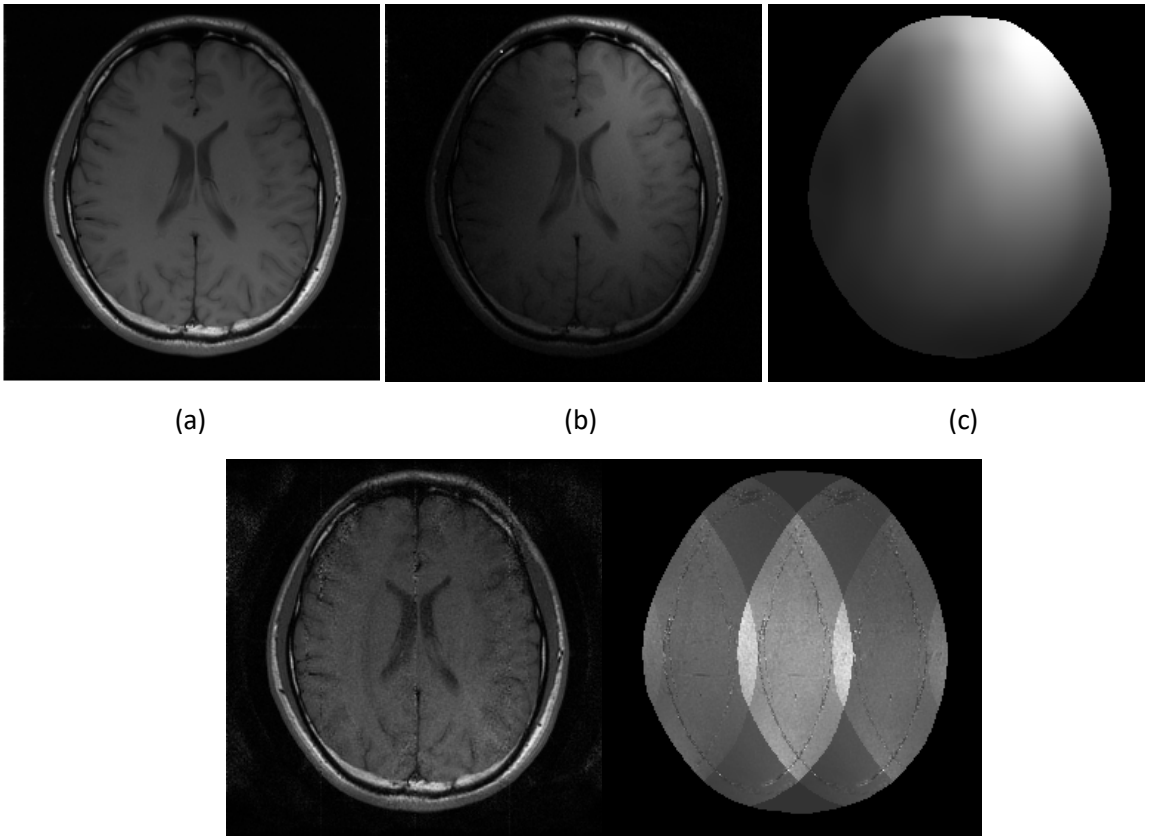

(a) (b) (c)

(d) (e)

Figure 2. The original brain MR image 1 (a), one coil image (b), the coil sensitivity map (c) related to the coil image (b), reconstructed image by SENSE (d), and g-factor map (e) with noise distribution in (d).

In addition, different numbers of pixel samples are randomly selected from 256 x 256 MR images each time for a trial. For the gray value of each pixel selected at each time, 8 neighbor pixel gray values are combined with this center pixel gray value are to obtain a feature vector to represent noisy level in the local 3 x 3 window. Feature vectors corresponding to the selected pixels are fed into perceptron classification algorithm in real-time. According to misclassification rate each time, classifier is dynamically adjusted based on the algorithm presented in the above section. For each time, the online cumulative mistake rates are list in Table 2. There are 30 times of trials in a sequence for the noise and non-noise pixels classification for both of brain images. Different brain image with different selection of threshold produces different cumulative mistake rate in real-time classification. For example, MR brain image 1 is T1 weighting, whose cumulative mistake rate is around 15% along 30 times of trials when g-factor threshold is set as 1.0, as indicated in the second column of the Table 2. The mean value

is 15.1% and the standard deviation is 0.2%. Similarly, for other configurations of g-factor thresholds on both of brain image 1 and image2, each column shows changes of cumulative mistake rates of online classifications. The mean values are 26.6% (brain image 1 with g-factor threshold 1.5), 29.2% (brain image 1 with g-factor threshold 2.0), 21.2% (brain image 2 with g-factor threshold 1.0), 38.5% (brain image 2 with g-factor threshold 1.5), and 21.0% (brain image 2 with g-factor threshold 2.0), respectively. The standard deviations values are 0.2% (brain image 1 with g-factor threshold 1.5), 0.2% (brain image 1 with g-factor threshold 2.0), 0.2% (brain image 2 with g-factor threshold 1.0), 0.2% (brain image 2 with g-factor threshold 1.5), and 0.2% (brain image 2 with g-factor threshold 2.0), respectively.

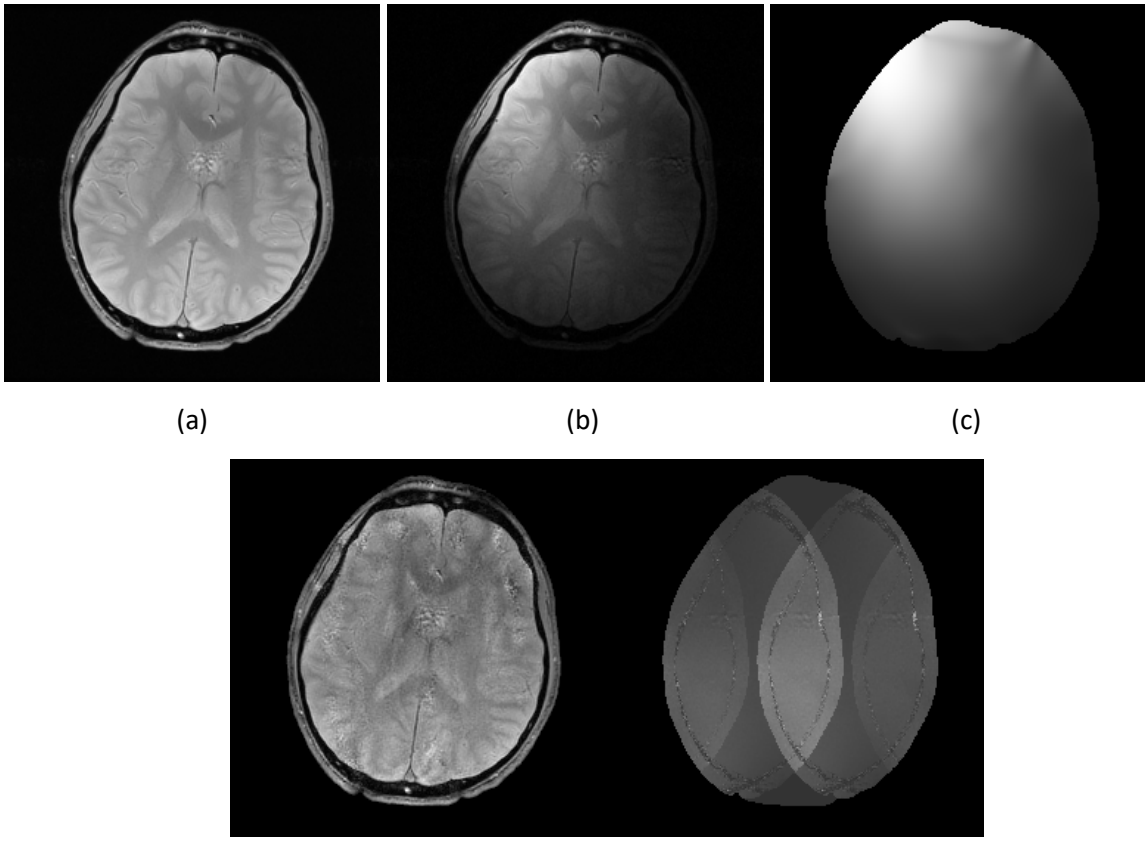

(a) (b) (c)

(d) (e)

Figure 3. The original brain MR image 2 (a), one coil image (b), the coil sensitivity map (c) related to the coil image (b), reconstructed image by SENSE (d), and g-factor map (e) with noise distribution in (d).

Table 2. Classification of noisy pixels with different noisy levels for two brain MR images shown in the Figure 2 and Figure 3. Cumulative mistake rate is used as the measure.

	Brain1, g1.0	Brain1, g1.5	Brain1, g2.0	Brain2, g1.0	Brain2, g1.5	Brain2, g2.0
t-1	15.149%	26.717%	29.364%	20.941%	38.040%	20.943%
t-2	15.079%	27.048%	29.190%	21.555%	38.597%	21.115%
t-3	14.838%	26.572%	29.149%	21.008%	38.396%	21.344%
t-4	15.007%	26.720%	29.155%	21.478%	38.750%	21.204%
t-5	14.772%	26.735%	29.303%	21.329%	38.512%	20.555%
t-6	14.742%	26.859%	29.109%	21.388%	38.156%	20.789%
t-7	15.121%	26.134%	29.442%	21.545%	38.608%	20.970%

t-8	15.396%	26.620%	29.514%	20.657%	38.449%	21.111%
t-9	14.879%	26.324%	29.181%	21.133%	38.237%	20.825%
t-10	14.844%	26.254%	29.002%	21.021%	38.155%	20.946%
t-11	15.245%	26.485%	29.404%	21.164%	38.361%	21.207%
t-12	15.033%	26.271%	29.105%	21.037%	38.210%	20.920%
t-13	14.944%	26.825%	29.184%	21.136%	38.242%	20.961%
t-14	14.986%	26.651%	29.280%	21.359%	38.777%	20.956%
t-15	15.271%	26.685%	29.185%	21.088%	38.599%	21.037%
t-16	15.439%	26.506%	29.512%	21.690%	38.560%	21.042%
t-17	15.337%	26.717%	29.366%	21.701%	38.449%	21.104%
t-18	15.329%	26.762%	29.282%	21.364%	38.411%	21.033%
t-19	15.254%	26.700%	29.239%	21.295%	38.542%	21.086%
t-20	14.899%	26.526%	29.523%	21.124%	38.644%	21.193%
t-21	15.034%	26.602%	29.065%	21.465%	37.958%	21.071%
t-22	15.237%	26.253%	29.147%	21.214%	38.513%	21.054%
t-23	15.048%	26.869%	29.181%	21.371%	38.492%	20.932%
t-24	14.996%	26.228%	29.172%	21.263%	38.765%	21.266%
t-25	14.706%	26.265%	29.312%	20.985%	39.008%	20.862%
t-26	15.248%	26.520%	28.920%	21.245%	38.214%	21.362%
t-27	14.871%	26.497%	29.221%	21.448%	38.733%	20.950%
t-28	15.408%	26.604%	29.543%	21.097%	38.286%	20.964%
t-29	15.219%	26.674%	29.182%	21.176%	38.402%	21.062%
t-30	15.228%	26.752%	29.175%	21.074%	38.475%	21.158%

5 Conclusion

An online learning algorithms is applied for classifying noisy pixels of MR brain images. The real-time perceptron algorithm enhances speed of noise classification in SENSE MR images, which have been widely used on clinical applications. Classifier parameters are dynamically updated based cumulative mistake rate produced each time during the classification procedure. In addition, real-time classification is able to provide quick noise information. For the future work, multi-class perceptron algorithms will be investigated to identify multiple levels of noises in the dynamic MR images.

REFERENCES

[1] Gondara, L, *Medical image denoising using convolutional denoising autoencoders*. Data Mining Workshops (ICDMW), IEEE 16th International Conference on 2016.

[2] Kohan, M.N., et al., *Denoising medical images using calculus of variations*. Journal of Medical Signals and Sensors, 2011. 1(3): p. 184-190.

[3] Seetha J., et al., Denoising of MRI images using filtering methods. Wireless Communications, Signal Processing and Networking (WiSPNET), International Conference on 2016.

[4] Shen, D., *Deep learning in medical image analysis.* Annual Review of Biomedical Engineering, 2017. 19: p. 221-248.

[5] Zhou, S.k., *Medical image recognition, segmentation and parsing: machine learning and multiple object approaches.* The Elsevier and Miccai Society Book Series, Academic Press 2016.

[6] Guido, T., et al., *Model attraction in medical image object recognition.* Proceedings of the SPIE, 1995. 2436(1): p. 18-29.

[7] Olesen O.V., et al., *Motion tracking for medical imaging: a nonvisible structured light tracking approach*. Medical Imaging, IEEE Transactions on, 2012. 31(1): p. 79-87.

[8] Lim J.H., et al., Motion tracking in medical images. Biomedical Image Understanding, Methods and Applications, 2015.

[9] Huang C., et at., Real-time 3D motion tracking using MR micro-coils for PET imaging. The Journal of Nuclear Medicine, 2013. 54(2): 44.

[10] Cleary, K., et al., *Image-guided interventions: technology review and clinical applications.* Annual Review of Biomedical Engineering, 2010. 12: p. 119-142.

[11] Shalev-Shwartz, S., *Online learning and online convex optimization.* Foundations and Trends in Machine Learning, 2011. 4(12: p. 107-194.

[12] Hoi, S.C.H, *LIBOL: a library for online learning algorithms*. Journal of Machine Learning Research, 2014. 12(1): p. 495-499.

[13] Pruessmann, K.P., et al., *SENSE: sensitivity encoding for fast MRI.* Magnetic Resonance in Medicine, 1999. 45(2): p. 952-962.

[14] URL: http://www.mr-tip.com/serv1.php?type=cam.

[15] Rosenblatt, F., *The perceptron: a probabilistic model for information storage and organization in the brain*. Psychological Review, 1958. 65(6): p. 386-408.

[16] Cesa-Bianchi, N., et al. *A second-order perceptron algorithm*. SIAM Journal on Computing, 2005. 34(3): 640-668.

[17] Pieciak, T., et al., *Non-stationary rician noise estimation in parallel MRI using a single image: a variance-stabilizing approach*. Pattern Analysis and Machine Intelligence, IEEE Transactions on, 2017. 39(10): p. 2015-2029.

[18] Aja-Fernandez, S., et al., *Statistical noise analysis in GRAPPA using a parametrized noncentral Chi approximation model.* Magnetic Resonance in Medicine, 2011. 65(4): p. 1195-1206.

AIVP ADVANCES IN IMAGE AND VIDEO PROCESSING
SOCIETY FOR SCIENCE AND EDUCATION UNITED KINGDOM
VOLUME 5, ISSUE 6
ISSN 2054-7412

A Mass Mediated Interpretation of The Chinese "Belt & Road Initiative" As Strategic Intelligence Perspective

[1]James A. Schnell, [2]Brian L. Schnell
[1]Ohio State University, USA
[2]Case Western Reserve University, Cleveland, Ohio, USA
james.schnell@fulbrightmail.org

ABSTRACT

This paper contrasts the current Chinese "Belt and Road Initiative" (BRI) against the opening of the U.S. west in the 19th century using principles of western rhetoric as basis for interpretation. Most specifically, Kenneth Burke's Dramatistic Pentad is used for initial clarification along with explanation of how further understanding can be realized via Fantasy Theme Analysis to better appreciate the expression of rhetorical vision. Recognition of how BRI can be understood differently, depending on the cultural context, is stressed as a strategic intelligence perspective. This is couched in the contextual framing of mass media influences as explained by Marshall McLuhan.

The Chinese "Belt and Road Initiative" (BRI) is a huge sweeping endeavor that will take years to conceptualize and fully implement. It envisions connecting many countries across multiple continents. It has parallels with how the U.S. opened lands that were west of Chicago in the 1800s, lands that extended to the Pacific Ocean. This paper contrasts the present-day Chinese "Belt and Road Initiative" against the opening of the U.S. west in the 19th century using principles of western rhetoric as basis for interpretation.

In doing so, the reader will recognize how such phenomena can be understood in varied ways depending on the cultural frame of reference. Hence, I seek to clarify what these events are and, more importantly, what these events represent. It is with the latter that I find considerable room for understanding and misunderstanding to occur. There are relevant facts to be recognized but, equally important, there are significant variables that are merely open to interpretation. Cultural perspectives are key with these interpretations as are the mass media channels that impact our understanding of such variables.

The role of mass media channels, in framing our understanding of the world around us, is gaining emphasis with the continued evolution of the information age and commensurate new communication technologies. We are finding that such new communication technological innovations not only enhance conveyance of meaning but that they impact our understanding of the phenomena being communicated about. That is, the new communication technologies impact the speed and format with which we receive information and they impact what is being reported on as result of that immediacy and format.

With the world becoming more interconnected we find ourselves encountering a phenomenon that has been historically less common but is becoming more common with increasing frequency. Most namely, that peoples who have rarely been in contact with each other in the past are now dealing

DOI: 10.14738/aivp.56.4107
Publication Date: 31st December, 2017
URL: http://dx.doi.org/10.14738/aivp.56.4107

with each other on a frequent basis via business, travel, education and popular culture venues. What goes on in one culture, indeed, has impact on other cultures. Such evolutions have great potential for not only opening doors to new understanding but for also have potential for creating misunderstanding. Mass media channels are part of such processes.

Fundamental in such processes is that we tend to interpret developments in other cultures via the mindset of our own culture. Such an approach can offer a perspective for understanding but it may not equate with how the culture being interpreted, in fact, interprets itself. This is the case with the "Belt and Road Initiative" that is underway in China.

China's president Xi Jinping announced creation of the BRI in 2013. It is intended to reorient relations among China and other countries in the Eurasian community. There are two aspects of BRI: an overland "belt" connecting China with Central Asia, Russia, South Asia, and Europe and a maritime "road" linking Chinese ports with those in Southeast Asia, South Asia, Africa, the Middle East, and Europe. It is intended to project an extensive network "of railways, highways, ports, pipelines, and communication infrastructure spanning the Eurasian continent and facilitating trade, investment, and people-to-people exchange. In 2015, Beijing announced a plan to develop six economic corridors to advance this initiative. China's leadership has rallied behind BRI, pledging substantial investment, creating new financial institutions such as the Asian Infrastructure Investment Bank and the New Silk Road Fund, and making diplomatic commitments to countries along the proposed routes" (Clarke et al, 2017, p. 66).

Announcement of BRI has stimulated considerable interest in the global community. A driving aspect of such inquiry grows from the question of what BRI means for each nation directly in the BRI path and the rest of the world order on other continents. As such, U.S. constituencies have been quick to interpret BRI in relation to phenomena familiar to the U.S. national mindset, which grows out of the western rhetorical tradition. Most notably the Marshall Plan that was stressed by the U.S. after World War II when the U.S. helped to rebuild war torn Europe. It helped to rebuild Europe and extend U.S. influence in the region. Such a context can be used to view how "China's Belt and Road Initiative is one example of an effort to accumulate influence far from Chinese territory. Supporters of the initiative explain that 'the New Silk Road can be understood as a type of Marshall Plan with Chinese characteristics; it reassures the Middle Country's neighbors, contributes to their growth and places them in a system designed by Beijing'" (Cooper & Shearer, 2017, p. 309).

BRI will require considerable resources from the Chinese government—resources that could be used with other needs within China. This situation is mildly exacerbated by the reality that it is something of a gamble that may not fully benefit Chinese people in intended ways. Hence, there may be pockets of people within the Chinese order who are lacking enthusiasm for BRI. Overall though, the Chinese people have embraced this extensive undertaking that has the potential to reshape the global economy. "As the Chinese writer Lu Xun once said, Chinese people opt for moderate reform in the face of revolutionary change. If you want to open a window against the darkness, you are likely to be rejected, but if you say you want to remove the rooftop for light, you will get the window opened" (Li, 2017, p. 73).

China's advance with BRI somewhat replicates past moves by Great Britain and the United States. The expansion of the British empire in the 1800's was perpetuated, in part, by the desire to create outlets for the British goods and capital that could not be utilized in the British domestic economy. The United States, in a similar manner, engaged in commensurate empire building via the same view that America's continuing economic growth required profitable export of American capital and

goods. China is confronted with a paralleled challenge of insufficient demand for its products and problems linked to minimal potential for domestic investment. As a result, using the British and U.S. as guide, China is pursuing to promote new markets beyond their borders. Extension of such new markets typically involves extension of geopolitical reach in that the new lines of global extension require protection. One can expect such context may serve as rationale for the projection of Chinese military capabilities (Layne, 2017, p.29).

Cultural imperialism often goes hand in hand with economic and militaristic imperialism. BRI will connect 68 countries from Southeast Asia to Europe and Africa. This has the potential to perpetuate a form of global culture that gives first billing to Chinese cultural components. The Chinese film industry will be one of the key cultural components. "We do not see Belt and Road's impact on culture and entertainment yet as communication with these countries has only just begun. But once the hardware is ready, the cultural impact will follow," says Professor Anthony Fung, co-director of the Hong Kong Institute of Asia-Pacific Studies at the Chinese University of Hong Kong (Chow, 2017, p. 16).

Enthusiasm for exporting Chinese culture into foreign markets has not always been met with enthusiasm for importing it. For example, there has been criticism that the Confucius Institute serves little more than Chinese propaganda functions under the auspices of promoting awareness of Chinese culture around the world. The film industry has the potential to enjoy better success. However, even with significant growth of the Chinese film sector, minimal success has been realized at the box office. Zhang Yimou's elaborate "The Great Wall" offers illustration, regarding Chinese films, in that it received minimal fanfare in relation to the extensive resources that were expended in production of it (Chow, 2017, p. 18).

The role of vision with BRI will be key. That is, BRI is an abstract construct that will involve many constituencies interpreting BRI in relation to what BRI means for them. At the same time, it will be important to concurrently have a fundamental foundation from which all parties recognize relevant variables. Historical context will be part of that foundation.

"On November 15, 2012, the day he became general secretary of the Chinese Communist Party, Xi Jinping stood onstage at the Great Hall of the People, in Beijing, to reflect back on his country's 5,000 years of history. After citing China's 'indelible contribution' to world civilization, Xi called for 'the great revival of the Chinese nation'" (Economy, 2017,

p. 141). This glorified past is drenched with images from periods when China led the world with advanced thought, power and resolve. Previous leaders—including Mao Tse Tung, Hu Jintao, Jiang Zemin and Deng Xiaoping—also reminded Chinese citizenry and the world of China's esteemed place in world history. In building upon this honored past Xi "has put in motion a massive infrastructure plan, the Belt and Road Initiative, which is designed to revive the ancient Silk Road and the maritime spice routes that flourished as early as the Han dynasty, thus reinforcing the claim of Chinese centrality. He has also articulated the idea of a 'new type of great power relations,' whereby China would enjoy the status of a global power on par with the United States" (Economy, 2017, p. 141).

One can infer parallels between U.S. President Donald Trump's call to "Make America Great Again" and China's harkening to a glorified past—hence "Make China Great Again." As observed in the 2016 U.S. presidential campaign, such proclamations to "Make America Great Again" can have far reaching effects. Trump won the U.S. presidency via that rallying call to the American electorate.

In such cases one can see large scale examples where entire segments of the U.S. population voted for leadership that would undercut their own individual economic well-being in favor of the perpetuation of national pride. Such nationalistic messages can inspire the public to move in unpredictable directions within a short amount of time.

The larger context of the 2016 U.S. presidential election offers more intrigue in that the same electorate that had elected Barack Obama in 2008 and 2012, in turn, elected Donald Trump. Obama is considered to be to the far left of American politics and Trump is considered to be at the far right of American politics. This evidences the degree of vacillation that can exist in U.S. politics and underscores some of the attributes of such a multi-cultural society with so many political interests to consider.

The election of Trump was practically unparalleled in modern U.S. political history. Virtually no well-established American polling organizations foresaw a Trump victory. He seemed to tap feelings of frustration and desire among the American populace in a manner that paved the way for him to personify America's greatness. In similar ways, President Xi can be recognized as the embodiment of China's path to, or reclaiming of, greatness.

The rhetoric put forth by Xi implies that BRI is merely a manifestation of China living out past themes in contemporary global relations. "This story has gone largely unchallenged. Yet two fascinating new books—Howard French's Everything Under the Heavens and John Pomfret's The Beautiful Country and the Middle Kingdom—suggest that there is much more to the story. French's book raises important questions about the accuracy of the rejuvenation narrative" (Economy, 2017, p. 142). Such challenges from historians will be part of the process of establishing historical legitimacy as BRI moves forward from idea to implementation.

Other types of challenges will be part of the BRI evolution. Many of these will grow out of the mere interpretation of what BRI is and what it means for the constituent. As noted earlier, U.S. entities have been quick to interpret BRI in relation to phenomena familiar to the U.S. national mindset, which grows out of the western rhetorical tradition. Kenneth Burke, the most prominent western rhetorician of the 20th century, offers a theory of Dramatistic Rhetoric that can be used as framework for interpreting BRI that exemplifies how the U.S. might come to understand BRI. Such an understanding could be foundation for U.S. thinking and subsequent actions.

A fundamental premise of Burke's rhetorical perspective stresses a "new rhetoric." New Rhetoric emphasizes "identification" between sender and receiver rather than "persuasion" done by the sender to the receiver. That is, the sender should seek to identify his/her needs with those of the audience. Burke builds upon this by describing dramatism--which is the study of human relations and motives using clusters and terms (elements) along with their functions. He clarifies his perspective, in a more detailed manner, by stressing use of a Dramatistic Pentad to interpret events.

The Dramatistic Pentad is composed of five elements: act, agent(s), scene, agency and purpose. The "act" is the conceptual center that other elements revolve around. The "agent(s)" are the individual(s) involved in the act. The "scene" is the situation. The "agency" is the means to the end. The "purpose" is the objective. Ultimately, an ACT takes place only when there is an AGENT who operates in a SCENE or situation, and employs an AGENCY or means to accomplish a PURPOSE (Golden et al, 2011, chapter 13).

The following describes how an American view of BRI can be deduced using the Dramatistic Pentad to frame BRI.

1. ACT - The Chinese government is promoting the Belt & Road Initiative to connect 68 countries from Southeast Asia to Europe and Africa to enhance economic, cultural and political development.

2. AGENTS - Include the Chinese government leadership, leaders of the other 67 countries in Southeast Asia, Europe and Africa located in the path of the proposed Belt & Road, the people of China and leaders of other major world powers.

3. SCENE - The situation involves Chinese advancement of BRI and reaction to BRI by the other 67 countries directly impacted by BRI and other major world powers.

4. AGENCY - The means stresses two aspects of BRI: an overland "belt" connecting China with Central Asia, Russia, South Asia, and Europe and a maritime "road" linking Chinese ports with those in Southeast Asia, South Asia, Africa, the Middle East, and Europe. It is intended to project an extensive network "of railways, highways, ports, pipelines, and communication infrastructure spanning the Eurasian continent and facilitating trade, investment, and people-to-people exchange. In 2015, Beijing announced a plan to develop six economic corridors to advance this initiative. China's leadership has rallied behind BRI, pledging substantial investment, creating new financial institutions such as the Asian Infrastructure Investment Bank and the New Silk Road Fund, and making diplomatic commitments to countries along the proposed routes" (Clarke et al, 2017, p. 66).

5. PURPOSE - To return China to its historic role as a global leader and reaffirm the place of Chinese culture as an advanced civilization on the world stage.

Using the Dramatistic Pentad interpretation of BRI as foundation, the western perspective can be elaborated on through analysis of rhetorical vision via Fantasy Theme Analysis, as clarified by Lu Xing (2008, pp. 112-113). Rhetorical vision involves a compilation of desired themes that unfold into an imagined form of reality in the minds of participants. Participants will function together, and individually, in accord with their shared understanding of this imagined form of reality. A convergence occurs through a shared view of goals, objectives, function and future. This analysis acknowledges consistencies of behavior and highlights how these consistencies lead to a constructed form of reality for participants as manifested in shared desires, intentions and meanings. Ultimately, this socially constructed form of reality provides direction for the perceptions of participants. Three themes can be delineated within this process. They focus on characters, actions and settings. A detailed understanding of the rhetorical vision can be realized by coding the characters, actions & settings and then constructing the rhetorical vision from these themes. Hence, the rhetorical vision maintained by each BRI constituent can be understood using this analytical process.

This application provides understanding of an American view of the Chinese BRI using principles of western rhetoric to frame BRI in a detailed manner. Such a view reflects the western rhetorical tradition and, as such, does not offer global understanding of BRI. BRI is a multicultural phenomenon due to the many cultures impacted by BRI and, as such, the understanding of BRI will be a multicultural event.

The Chinese BRI has many parallels to the opening of the west that went on in the U.S. during the 19th century. This was often referred to as "manifest destiny." Like China, prior to the opening of the west, much of the U.S. population lived in the eastern part of the country. The movement west was as a movement toward the new and somewhat unknown. All kinds of potentials but all kinds of risks, as well.

The American west, in the 1800's, represented the future. Hence, the phrase "Go west, young man" was echoed many times in that it encouraged youth to look toward a new and exciting future involving such things as the California gold rush, the creation & settling of the western states, land claims and considerable development. One can see similar parallels with the opportunities and challenges associated with the opening of the Chinese western provinces.

Such development is romanticized in the history of 19th century America. It was a time of excitement, potential and vision. However, lesser considerations are given to those who lost during the process of adventure and settlement—or should I say resettlement. Most notable, in this regard, are the Native Americans who were forcibly removed from the lands that were being "opened" via white settlement. The history of my own ancestors illustrates how this occurred in that time frame.

My family background is a mix of German, Polish and Native American. My father's last name is Schnell. My father's side of the family are from an Amish-Mennonite farming community in northeastern Ohio (Berlin, Ohio). As is custom I carry the last name Schnell, from my father, but I grew up among my mother's people closer to central Ohio (Gahanna, Ohio).

My mother's side of the family carry the last name Sandusky. The Sandusky family lineage is part of the Sandusky Indian heritage that was linked to the Wyandotte Indians who were, in turn, a sub-unit of the Huron Indians. These Indians inhabited what become known as the Ohio River Valley.

For the most part, my Native American ancestors that survived that period (some had been killed outright) were forcibly removed from central Ohio to Indian reservations in Oklahoma. Some, most directly linked to my lineage, were kept in Ohio under the auspices of a form of involuntary servitude. That is, to provide cheap labor that was essential for developing the area for white settlement. Over the years, primarily through inter-marriage with the occupying white population, the Sandusky Indians managed to assimilate into the white society and minimize the stigma associated with our Native American roots.

I share this illustration to exemplify how the story of the "opening" of the American west can be romanticized as some type of glorious event but it is a blood-stained chapter in American history. The romanticized nature of this occurrence illustrates how strong the power of vision can be in the public mind. It can almost seem as if God, or some divine entity, sanctioned the opening of the American west whereas it really was a murderous bloodbath that unleashed painful horrors on those who were in the path of economic development. It is a common story that is retold throughout the history of expanding civilizations.

Interpretation of westward expansion via the "manifest destiny" vision in the U.S. can be easily achieved using the Dramatistic Pentad just as has been done to interpret the Chinese BRI.

The following describes use of the Dramatistic Pentad to frame westward expansion in the U.S.

1. ACT – The U.S. was a relatively young country just beginning to realize future potentials and the means for moving toward achievement of those potentials. Much of this young country was settled along the eastern border—in areas where those coming from Europe had arrived into this new land. Westward expansion was the logical expression of the U.S. destiny.

2. AGENTS – Included white settlers, U.S. government representatives and businessmen. Native Americans had something of a muted role to play in this drama in that they represented the past rather than the future.

3. SCENE – This unfolding drama fit well with the American family framework. Young, restless, adventuresome, strong and capable. The young country was full of aspiring people who heeded the call to continually move west from the eastern population centers. As areas were settled, these new settlements were used as launching pads for further movement westward. The Lewis & Clark expedition westward captured the imagination of those back east. Eventually this movement westward landed on the west coast of (what is now) California, Oregon and Washington. At that point, the long reach westward then began to focus attention on domesticating the land that had been claimed. Such domestication involved the establishment of railroads, telegraph lines, small towns became cities and the land was tamed.

4. AGENCY - The means, that was outlined within the scene, took on fuller expression via more thorough development. The American cowboy era exemplified the rugged individualism that manifested the "wild west." Over time, the means for progress was recognized via a more domesticated form of individualism that stressed planned growth and future oriented thinking centered on building civilized population centers. This was concurrently addressed with an eye toward preserving the natural beauty inherent in, what became, the western states. This process has not yet been completed. The modern centers of life in the U.S. are very much found on the east and west coasts of the country and then between the east coast and Chicago. Otherwise, much of the lands between Appalachia to Montana are still in the process of being developed on par with the more well-established population centers of the east and west coasts.

The state of Texas best illustrates a land in transition along these lines. Dallas, San Antonio and Houston have developed into large urban population centers while the rest of the state is moving toward such modernization. The role of the rugged individualist spirit is still embraced in this transition via the rich embodiment of the Texas cowboy. One will even notice cowboy hats fashionably worn by wealthy businessmen in Dallas, Houston and San Antonio. Image can be larger than life.

5. PURPOSE – To establish the U.S. as "land of the free and home of the brave." That is, the rhetorical vision that is promoted seeks to exemplify how the American spirit (free enterprise, innovation and hard work) can be a force of nature in the development of largely unsettled lands. It is meant to be a beacon for the rest of the world that has been associated with religious forces of divine intervention. That the U.S. was, and has continued to be, a land of immigrants is part of this rhetorical vision. One will clearly observe, throughout the history of the U.S, that there are far (far) more people seeking to immigrate into the U.S. than to immigrate away from it.

A factor in this, that is minimally acknowledged, is the role of religion. Is only vaguely alluded to from the U.S. perspective and it is entirely absent from the Chinese perspective, as earlier depicted in the Dramatistic Pentad interpretations. However, it is worth engaging in closer scrutiny to find elements that suggest consideration for divine intervention.

The role of a Christian God is indirectly asserted throughout the opening of the west in the U.S. "In God We Trust" can be found on U.S. currency, churches were a staple (along with saloons) in towns across the plains, babies were typically baptized at birth and ministers solemnized weddings. That the light of God shone brightly over the lives of westward settlers was clearly implied.

The role of religion with the Chinese is practically absent, especially in modern day China, in relation to the governmental discouragement of religion. Chinese leader Mao Tse Tung referred to religion as

the "opium of the masses." However, a view of Mao as a supernatural being can be recognized within Chinese culture.

In 1995 I was on a visit to Beijing, China and turned off the bedroom light one night as I prepared to lay down to sleep. I laid in bed, about to doze off to sleep, and noticed a glowing in the dark at the foot end of my bed. It came from the floor. I could not see what was creating the glow, rather, I could only see the glow. I curiously crawled to the edge of my bed and could see the source of the glow was a bust of Mao Tse Tung.

I was creating a collection of Mao memorabilia at that time, especially busts of Mao. I soon learned that a few of the Mao busts I had collected glowed in the dark, as did some of the plastic Mao badges. I had never seen such a thing until I remembered back to my childhood when I had a couple plastic figurines of Jesus that glowed in the dark. The idea of a glowing entity seemed to imply some sort of supernatural being.

It then occurred to me that Mao was something of a political/nationalistic/spiritual icon. He was something akin to a supernatural god. I've talked to Chinese friends who have described how they were surprised when Mao died in 1976 because it was assumed he would live many years beyond the standard old age and that finding he was a mere mortal opened their eyes to the truth about his mortality. I believe that degrees of, what Americans view as, spirituality can be recognized in Chinese nationalism. Love of country in China is something akin to a spiritual love. This can be closely aligned with the notion of patriotism. However, patriotism and spirituality can be observed separately in the U.S.

The process of understanding phenomena presented in this report has become more complicated in relation to the new communication technologies associated with continually evolving information age mass media forms. Marshall McLuhan, the most prominent mass media theorist of the 20th century, explained this with his dictum "the medium is the message." That is, the technology that conveys information also, within itself, conveys meaning (Golden, 2011, chapter 20).

Inherent in his perspective is that our understanding of the world is altered by the media that are in effect at any given time. The media that surround us, that we use, convey meaning in—and of—themselves. This can be recognized via the different media that have existed throughout history.

McLuhan stresses this through consideration of four periods of media: tribal society, manuscript society, Gutenberg society and electric society. Tribal society stressed face to face communication. Manuscript society (0-1400 AD) occurred when ideas could be recorded in written form using words. Gutenberg society came into being with development of the printing press whereby ideas could be written, mass produced and distributed on a mass level (1500-1900 AD). Electric society (1900-present) exists with the use of electric circuitry (telegraph, telephone, TV, radio, computer etc.) in ways that resonate with the belief that such electric circuitry is an extension of the central nervous system.

Many of the meanings that evolve from this nexus of interpretation, cross-cultural framing and mass media interplay place us at a transformational point in history. Our understanding of the past, present and future are impacted as the notion of memory and context is altered. The future that we anticipate will not always be what we thought it to be. Hence the present will impact our understanding of the past and the present will impact our understanding of the future. The future will impact our understanding of all three: past, present and future.

We live in a time where there is a possibility for everything but little certainty of anything. The role of vision will help chart the future courses to be taken, understand present circumstances we find ourselves in and interpret from whence we came. As such, the learned person will do well to keep a pulse on the significance of cultural contexts and the evolving technologies that impact such cultural contexts.

REFERENCES

[1] Chow, V. "Silk Road May Boost Film Reach," Variety, September 9, 2017, pp. 16-18.

[2] Clarke, M., Small, A., Pant, H., Peyrouse, S., Roy, M., Kassenova, N. and H. Yu. China's Belt and Road Initiative: Views Along the Silk Road. Seattle, Washington: The National Bureau of Asian Research, 2017.

[3] Cooper, Z. and A. Shearer. "Thinking Clearly About China's Layered Indo-Pacific Strategy," Bulletin of the Atomic Scientists, Vol. 73, No. 5; 2017, pp. 305-311.

[4] Economy, E. "History with Chinese Characteristics: How China's Imagined Past Shapes Its Present," Foreign Affairs, July/August 2017, pp. 141-148.

[5] Golden, J., Berquist, G. and W. Coleman. The Rhetoric of Western Thought. Dubuque, Iowa: Kendall/Hunt Publishing Co., 2011. Tenth Edition.

[6] Layne, C. "Contemplating Decline: China's Challenge to America Percolates on Many Fronts," The American Conservative, July/August 2017, pp. 29-33.

[7] Li, A. "China Facing the Trump Presidency: Opportunities for Global Power Projection, Current Affairs, No. 2, 2017, pp. 69-73.

[8] Lu, X. "Construction of Nationalism and Political Legitimacy Through Rhetoric of the Anti-SARS Campaign." In Powers, J. and X. Xiao The Social Construction of SARS: Studies of a Health Communication Crisis. Philadelphia, Pennsylvania: John Benjamins Publishing, 2008.

AIVP ADVANCES IN IMAGE AND VIDEO PROCESSING
SOCIETY FOR SCIENCE AND EDUCATION UNITED KINGDOM
VOLUME 5, ISSUE 6
ISSN 2054-7412

Pedological Characterization of the Soils of Atbara and Gash Rivers Upper Atbara Project Area (Kassala State - Sudan)

El Abbas. Doka M. Ali[1], Neil R. Munro[2] and Karl Peter Kucera[3]
[1]Land Resources Consultant, College of Agricultural Studies, Sudan University of Science and Technology, Shambat.
[2]International Consultant, Soil Survey and Land Evaluation.
[3]International Consultant, Soil Survey and Land Evaluation.
adoka21@gmail.com; Neil.munro@dial.pipex.com; KpKucera@gmail.com

ABSTRACT

The soil study area is composed of wide and nearly flat alluvium plain deposits laid by Atbara and Gash Rivers. The study area makes about 751,290 ha and lies within arid and semi-desert climate zones and experiences rainfall in the order of 100 mm in its northern edge, increasing to some 400mm at its southern boundary close to Kassala and east of New Halfa town. The soil study was based mainly on a semi-detailed level soil surveys and the key specifications are a field density of 1 observation each 150 ha. Previously published soil study information was reviewed and incorporated in the findings [5[; [17]; [14].

The Aridisols and Entisols in eastern region of Sudan have high potential for crop production, but some constraints emerge affecting crop performance and decreasing yields. Those limitations are aspects of climatic conditions, parent materials and topography manifested generally in, 1) soil moisture deficiency and locally in; 2) accumulation of secondary salts 3) clayey topsoil textures. Aridisols are the soils of arid regions that exhibit at least some subsurface horizon development. They are characterized by being dry most of the year and limited leaching. Aridisols contain subsurface horizons in which clays, calcium carbonate, silica, salts, and/or gypsum have accumulated. Aridisols in their natural state are used mainly for range, wildlife, and recreation. Because of the dry climate in which they are found, they are not used for agricultural production unless irrigation water is available. Entisols formed by rapid deposition on floodplains are universally favored for growing food crops in large part because of the influx of fertility in the deposited material, their level topography, and often the proximity to transportation and water afforded by adjacent rivers. In aridic (torric) soil moisture regimes their alluvial deposits close to rivers are more easily irrigated than associated soils on adjacent higher terraces or the far away finer clayey deposits.

Many, if not most of these areas are subject to flooding and often have extremely abrupt textural differences (i.e. stratifications) engendered by sedimentation processes. In floodplains the river channels migrate as the watershed characteristics change leaving sandy and silty sediments (levees) near the riverbank and finer textured materials further from the riverbank. In aridic moisture conditions Entisols on depressional areas or at higher terraces close to Aridisols are subject to salt accumulation similar to Aridisols. To minimize the concurrence of hazards in Aridisols and Entisols, management procedures should adhere to land and crop management systems. As well, the fertility status is likely to decline due to intensive farming of some nutrient-depleting crops, but this nutrient

DOI: 10.14738/aivp.56.4148
Publication Date: 31st December, 2017
URL: http://dx.doi.org/10.14738/aivp.56.4148

deficiency is correctable through implementing a fertilizer programme. In the study area, some parameters are management-factors determining e.g. topsoil textures and flat slope favoring uniform distribution of irrigation water through well designed irrigation and drainage network. Those technical inputs if properly used and practiced are expected to sustain crop production.

Key words: Aridisols, Entisols, Atbara and Gash Rivers, Alluvium deposits

1 Introduction

The Upper Atbara study area is situated between Atbara River in the west and Gash River in the east with a total area of 751,290 ha. The area lies north of the asphalt road connecting Kassala and Khashm El Girba towns and extend northward further to north of Goz Ragab, Jebel Ufrek and Hadaliyah. As well along the eastern border of the area runs the highway which connects Kassala to Port Sudan. The area is nearly flat with relatively few water channels dissections in the south and predominantly windblown features in middle and northern parts. Khashm El Girba Irrigated scheme lies to the west of this area across River Atbara. The Gash River Delta which borders the area to the west comprises a large seasonal irrigated farming area (Gash Agricultural project). Figure 1 shows the location of the study areas [5].

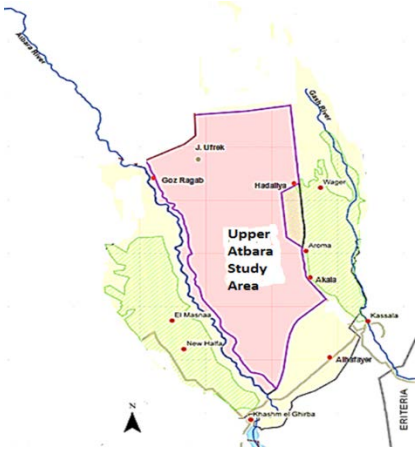

Figure 1: Location Map of Upper Atbara Study area. The map shows Atbara River, Gash River, New Halfa and Gash Delta Agriculture areas (Modified from [5])

Recent climatic maps showing the different climatic regimes in Sudan were produced based on the Papadakis climatic classification by [24]. The climatic zones (Figure 2) are based primarily on the water balance, using monthly rainfall and potential evapotranspiration data (Penman formula). The differentiating criteria are significant for agriculture, whilst the zones also correspond with natural vegetation zones. In this context two main climatic zones are defined, in which the climate of the northern parts of the study areas lie in the semi-desert zone (D3.1 or Zone 5) represented by Aroma Met station whereas the southern parts lie in the arid zone (A1.1 or Zone 4) represented by Kassala and New Halfa Met stations [25[; [9]. The following is a brief descriptive account of the main climatic parameters (Figure 2 and Table 1). At zone 4 the mean maximum temperatures of the hottest month (April and May) are 40.9-41.5 oC; whilst the mean minimum temperatures of the coldest month (December and January) are 16.5-18.8 Co. They are followed by a general rise of temperature in February and March. In summer the maximum exceeds 45 Co imposing extreme conditions of heat and dryness affecting the perennial vegetation, and the minimum is at 33-35 Co. At zone 5 the mean maximum temperatures of the hottest month (April and May) are 41.2-42.1 oC; whilst the mean minimum temperatures of the coldest month (December and January) are 14.3-15.6 Co. At both zones

December and January are followed by a general rise of temperature in February and March. In summer the maximum temperature slightly exceeds 45 Co imposing extreme conditions of heat and dryness affecting the perennial vegetation, and the minimum is at 33-35 Co. These conditions are relieved by the first rains of the new season.

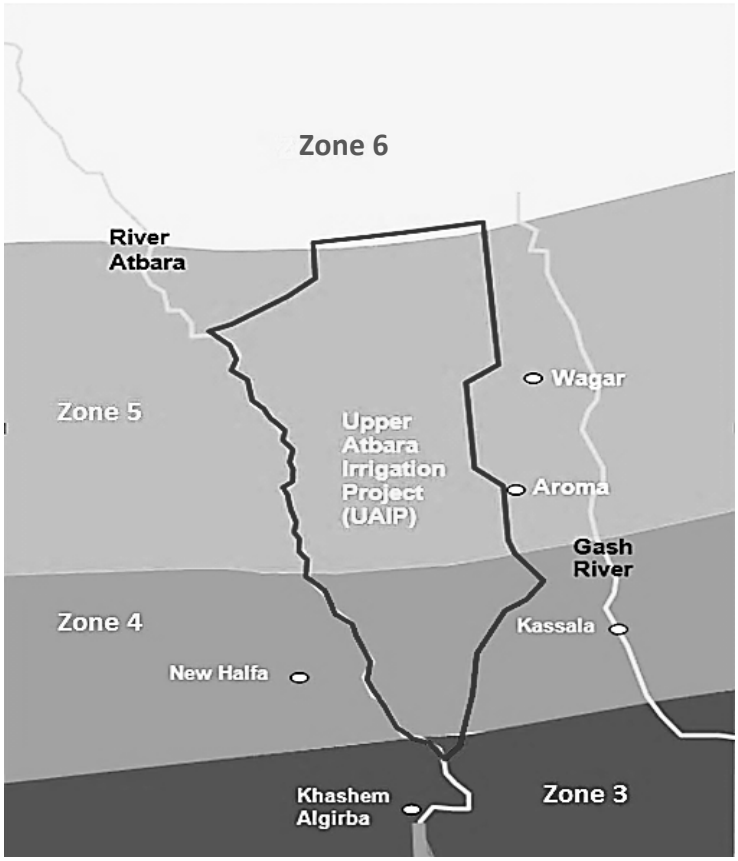

Figure 2: Climatic Zones 3, 4, 5 and 6 at Study area ([24] and [9])

The rainfall of the study area, being an integrated part of the central clay plain of the Sudan lies mainly within the arid and semi-desert climates (A1.1 and D3.1) of [24) and associated with the West Africa monsoon system, derived from South Atlantic and Congo air masses, with some Indian Ocean influence. The average annual total rainfall is about 235 and 175 mm at zone 4 and 5 respectively which falls mainly in the months of June–September, and is less than 44 per cent of the annual potential evapotranspiration. All the months are dry since the average rainfall never exceeds the potential evapotranspiration. Relative humidity being 25-60 % and 25% - 50 during most of the year rises to 70 per cent in the rainy season. As represented by Kassala and Aroma meteorological stations, the evapotranspiration exceeds the annual monthly rainfall indicating the dry conditions of the climate throughout Study area. This indicates that there is no humid month at study area and irrigated farming should be considered in the area. Supplementary irrigation might be possible during rainy season especially on slightly depressional or receiving sites.

Table 1: Monthly Rainfall and ETo in Zone 4 and 5 in Upper Atbara Irrigation Study area

Zone	(mm)	Jan	Feb	Mar	Apr	May	Jun	Jul	Aug	Sep	Oct	Nov	Dec	Yearly
4 Southern Parts of STUDY AREA (A1.1) Kassala	ETo (mm/ month)	180	193	248	255	263	264	236	211	207	223	207	195	**2682**
	Mean Monthly Rainfall	0	0	0	2.1	11	24.4	67.6	81.9	39.2	8.6	0.2	0.0	**235.0**
	Wind Prev. Direction	N	N	N	N	N	S	S	S	S	S	N	N	---
	Wind Mean speed Km/H	9	10	10	9	9	12	14	13	10	9	10	11	**10**
	R.H. %	45	39	31	27	30	38	54	60	53	40	39	45	**42**
5 Northern Parts of STUDY AREA (D3.1) Aroma	ETo (mm/ month)	127	137	186	189	195	204	192	183	171	158	144	130	**2,017**
	Mean Monthly Rainfall	0.6	0.0	0.0	2.5	9.1	16.8	58.8	51.9	26.3	6.2	0.8	0.0	**173**
	Wind Prev. Direction	NE	NE	NE	N	S	S	S	S	S	NE	NE	NE	--
	Wind Mean speed Km/H	4	4	5	4	4	6	6	5	4	3	4	4	**4.4**
	R.H. %	46	39	32	25	25	30	44	49	46	36	38	44	**38**
4 Southern Western Parts of STUDY AREA (A1.1) New Halfa	ETo (mm/ month)	298	196	254	273	267	276	239	211	207	192	189	171	**2772**
	Mean Monthly Rainfall	0.1	0.0	0.0	2.8	14.7	22.3	74.2	94.3	36.1	4.3	0.6	0.0	**249.5**
	Wind Prev. Direction	N	N	N	N	SW	SW	SW	SW	SW	N	N	N	---
	Wind Mean speed Km/H	10	10	10	10	9	12	13	11	9	6	8	8	**10**
	R.H. %	41	34	27	23	25	33	49	54	49	38	37	40	**38**

(Source: Sudan Meteorological Authority Database 1971- 2000)

The study area is flat with a reasonably constant gradient however, there are localized depressions and several shallow drainage systems running from east to west in which water ponds during and after the rainy season, particularly in the southern part of the area. Elevation decreases from approximately 475 meters above sea level (masl) at the southern boundary to approximately 400 amsl at the northern boundary, with an overall gradient of approximately 0.5 m per kilometer, but with a higher gradient in the southern half (approx. 0.8 m/km), and lower gradient in the north (approx. 0.3 m/km).

The study area is characterized by soils derived from two major geomorphologic units, namely the Gash River fan and Atbara Flood Plain [19];[20];[21];[22]; [12]. The Gash River fan can be subdivided into Very Old Gash Fan, Old Gash Fan and Sub Recent Gash Fan. Soils of the Sub Recent Gash Fan (Gash delta) overlie older Gash fan deposits and exhibit layering associated with sub recent and recent fluvial processes [6] Gash River is an intermittent river that floods annually and provides fresh sediment in active flood zones and through flash flooding. Flows in the Gash River have high velocity during peaks of rainy season and the river forms many channels, which can be clearly seen on the satellite imagery. According to our field experience, flooding of Gash River sometime reaches as far as Hadaliyah settlement and in several locations also floods land adjacent to the main north south road [23]; [5]..

The Atbara Plain consists of two major units namely heavily dissected kerrib terrace and Atbara Alluvial Plain with localized depressions generally adjacent to the kerrib deposits [27]. Since the commissioning of the Tekeze Dam in Ethiopia the Atbara River flows now throughout the year, and since the construction of the Khashm el Girba dam does not seem to cause regular flooding. Flooding or inundation takes place only as a backup behind the kerrib deposits for short periods during heavy rainfall events during the rainy season. Atbara plains consist of very flat terrain (< 1 %) with some buried channels. The Atbara River is confined to a channel formed by kerrib lands - former levees and terraces that form prominent highly dissected physiographic feature of the area landscape. This unit is elevated above the general level of the former flood plain and highly dissected through gully and rill erosion. There are some localized flat sections of the terraces suitable for smallholder pump irrigation for production of vegetables and fruits.

Natural vegetation and Present land use

The plant community in study area consists of a mix of Acacia tortilis(Samr), Acacia raddiana(Seiyal), and Acacia mellifera(Kitr), withscattered Acacia nubica(Laot),Balanitesaegyptiaca(Heglig),Capparis decidua (spinosa) (Tundub), Bosciasenegalensis(Mokheit)and open areas of grasses and herbs. Acacia tortilis and Acacia raddiana are continuously being browsed by camels and goats and because of this they are not destroyed. Balanitesaegyptiaca is widespread in the area forming parkland. The most abundant grasses include Aristidamutaiblis, Aristidapallida, Cenchrusbiflorus, Maeruacrassifolia and Cymbopogon proximus [15] and [5]). The Vegetation on floors of water channels includes large trees of Acacia ehrenbergiana(Salam),Capparis decidua(Tundub) and Acacia raddiana(Seiyal).At the Kerrib land Acacia nilotica (Sunt), Acacia nubica (Laot), Acacia raddiana (Seyal) are the most abundant species.Some parts of the study area have sporadicrainfed farming, mostly sorghum. Much of this is undertaken villagers from surrounding villages. A considerable number of grazing animals and nomadic tribes were noticed all over the area and most probably they come at the end of the rainy seasons to look for water which is retained in Hafirs for quite some time.

2 Materials and Methods

A total of 4328 augers and 379 profile pits were made (Figure 3).The locations of all pit and auger sites are demarcated on Landsat images. These locations are based on GPS co-ordinates and shown on figure 3. Field recording of soil auger sites and soil profiles was on standardized proformas and soils were described following the [8] “Guidelines for Soil Description”. The observations included [5]:

- Auger number; Surveyor; Date; GPS co-ordinates; Landform; Topography; Slope; Site; Surface Features; Termitaria; Trees; Shrubs; Land Use; Water-table; Soil drainage class; Samples; Soil type; Depth of cracking; Soil code; Soil horizons (for each: boundary, colour, colour code, mottles, texture class, cracks, clay skins, slickensides, coarse fragments, reaction to dilute hydrochloric acid, calcium carbonates, iron-manganese, gypsum, and other recorded features).At all auger sites soil samples were collected from the 0.0-0.3, 0.3-0.6 and 0.6-0.9 m depths, for pH, salinity (EC) and sodicity (SAR) screening.

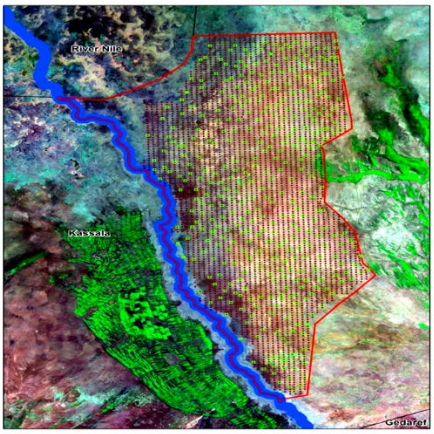

(Source: DIU 2014)

Figure 3: Sites of Soil Augers (Red dots) and Profile Pit Observations (Green squares) in study Area that are Demarcated on Landsat (October 2007).

3 Results and Discussions

3.1 ARIDISOLS

3.1.1 Surface Features and Morphological Properties

Aridisols are the dry soils of arid climates (the root arid or id comes from the Latin aridus for dry). In the study area during rainy season they receive enough rain to permit rainfed agriculture. They may have clay enriched subsoil and /or cemented to non-cemented deposits of salts or carbonates. Salinization or salt build up should be observed when using Aridisols for irrigated agriculture. A typical horizon sequence would be A, Bk, C. The diagnostic features are an ochric epipedon and an argillic, cambic, calcic or gypsic subsurface horizon (Figure 4).

3.1.2 Surface mulch and/or sealing

The surface mulch comprises fine and medium sized granules (2-5 mm) occasionally obscuring surface cracks in depressional areas. It is the first surface feature to be identified on the soils of the study area, and varies in thickness between 10-50 mm. The mulch is a water-conserving feature reflecting beneficial agronomic practices, such as harvesting of groundnuts, tubers and shallow-rooted vegetable and growing of food grain (sorghum and millet). Such cropped areas are relatively more in southern parts of study area. In irrigated farming, sprinkler irrigation may be more satisfactory because it would make gradual wetting possible and offers the possibility of structural improvement [11]. However, some of the fine textures do not form mulch on drying but produce "crusty surface". These crusty surface soils are commonly found in depressions or shedding sites. Surface runoff and wind erosion on sloping areas produced such sealed surfaces.

Figure 4: Aridisol profile (Vertic Haplocambids) at Study area

3.2 Aridic and Cambic properties

A surficial or near surface crust; a pavement of embedded and loose pebbles or of stones with a black to reddish brown desert varnish; shrinkage polygons, locally with the appearance of slick spots (takyr), with cracks continuing to or into the B horizon. Stratified and homogenized subsoils are common with variable topsoil textures (Figure 5). Water deficiency under natural conditions, is a problem, at times, in all Aridisols because taxonomic criteria dictate that they must have a layer characterized by salt accumulation ([16] and [17].A typical Aridisol has an even surface topography; with a thin surface mulch or sealed surfaces. Topsoil structures are moderate to strong with dominantly medium size sub-angular blocks. In Study area the Aridisols consist of flat mostly sealed surface in a continuous pattern of flat plains, or slightly raised areas with this mulchy surface masking the topsoil fissures and cracks. Several hypotheses have been put forward to explain the genesis and formation of Aridisols. These have in common that they relate most of their morphological features to the aridic moisture regime. They pointed out that they have some degree of soil formation in subsurfacehorizon (cambic horizon or stronger). Other important features include very limited amount of organic matter in topsoil (ochric epipedon) and a rearrangement in soil profile of more or less soluble salts (chlorides, sulphates, carbonates, silicates) into weak or strong, soft or cemmented forms (calcareous, calcic, petrocalcic,etc.). The soils may or may not have a degree of pedogenic textural differentiation (argillic horizon).

(A) Stratified with heavy texture topsoil

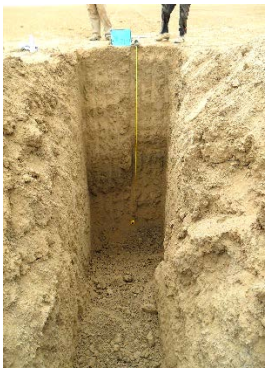

(B) Stratified with medium texture topsoil

(C) Homogenized top and subsoil

Figure 5: Soil stratifications and homogenization in some profiles at Study area Structure and other profile features(Source: [5])

3.2.1 Mineral concretions and aggregates

CaCO3 concretions and other forms of pedogenic carbonate have been described in profiles at the central and northern parts of Sudan [4]. In Aridisols the carbonate concentrations have been differentiated into types based on their appearance in thin sections. Carbonate has also been described from stereomicroscopic observation of undisturbed soil fragments and wet-sieved fractions over 0.5 mm and in soil profile walls. X-ray diffraction shows that in all samples the carbonate mineral is calcite [1]; [2]. Soft, powdery types of carbonate are diffused nodules or channel neo-calcitants; hard, discrete types are generally nodules, sometimes concretions, septaria and pedodes (Figure 6). The hard types have been differentiated on the presence and form of "impregnations" by iron and manganese (dendrites of manganese, neo- or quasiferans) and of cutans (generally manganese). Often there is a relation between types of pedogenetic carbonate present and other profile characteristics. Soft, powdery types appear to have formed in situ. Hard, discrete types in the accretion of the carbonate and formation of "impregnations" and cutans are due to processes which are – or have been- active in the lower part of the profile.

3.2.2 Physical properties

All soils are > 2.0m deep*. The Aridisols clay varies in depth from 2 to < 4.0m. The strata at the surface are heterogeneous brown, dark brown or dark yellowish brown silty clays, clay loams or sandy clay loams. Infiltration rate (permeability) and hydraulic conductivity tests were carried in the field. The values for untested (AWC) parameters were extracted from [10]. The infiltration tests were conducted in the study area using double ring infiltrometers. The values represent the basic infiltration rates which show almost consistent trends of 1.4 cm/h due to the behaviour of the homogenous soils of the study area. The optimum basic infiltration rates for surface irrigation are considered to be in the range of 0.7 to 3.5 cm/h, although acceptable normal values range from about 0.3 to 6.5 cm/h, [10]. However, it is reported that the methods of infiltration measurement can suffer from a number of errors including, lack of adequate pre-wetting of dry clayey topsoil that need weeks of pre-wetting before fissures and cracks are closed; and soil disturbance effects due to mulchy surfaces which may alter the soil - water intake characteristics.

3.2.3 Chemical and Mineralogical properties

It is assumed that the vertic (high clay content) or non vertic (Typic) Aridisols of any soil unit will have a similar chemistry to that soil unit since subsoil the control section determines the soil class and the topsoil. The soil particle size analysis recorded clay content in the range of 30-60% that belongs to the clayey and fine loamy classes in the FAO textural triangle and to the likely smectitic and Kaolinitic mineralogy. The CEC values are fairly consistent with this range of clay content [4].

The total nitrogen and organic carbon contents are very low ranging from 0.02 – 0.0 4 % to 0.6 – 0.8 % respectively indicating very low organic matter content that coincides with the amounts usually present in an arid climate. The available phosphorus, extracted with sodium carbonate buffered at pH 8.5, dominantly varies between 3 and 5 ppm with a few high figures up to11 ppm. Dominant amounts are deficient for most crops and questionable for cereals and grasses – Table 2. The availability of phosphorus is critical to plant uptake because soil alkalinity (pH 8.5 – 9.0) causes fixation and/or formation of insoluble compounds. However, crops vary in response and therefore the requirement for fertilizers application need to be assessed by field trials against the particular crop of interest after determining soil reactions.

Figure 6: CaCO3 nodules, concretions and aggregates in Aridisols of Study area

Table 2: General Interpretation of Available Phosphorus Analysed by Olsen's Method

Characteristic crop demand	Examples	Indicative available phosphorus values		
		Deficient	Questionable	Adequate
Low P	Grass, cereals, soybean, maize	< 4	5 - 7	>8
Moderate P	Lucerne, cotton, sweet corn, tomatoes	< 7	8 - 13	>14
High P	Sugar beet, potatoes, celery, onions	< 11	12 – 20	>21

(Source: Landon, 1991)

The soil reaction is alkaline varying between mildly to strongly alkaline in almost all of the soils of the area. The pH-paste values of the saturation paste profile data ranges from 6.5–9.5 with a mean of 7.9. These values tend to be higher with the increase of the soil: water ratio (dilution effect). In this respect, pH values exceeding 9.0 are occasionally found in the suspension 1:5 soil: water ratio. Although generally the reaction of the soil matrix is slightly or moderately to highly calcareous, the laboratory measured $CaCO_3$content ranges from zero to 3.7%. Higher contents are infrequent and occur in the substratum in some profiles.. Large fragments have little influence on soil fertility and it is the smaller particles, often found in the silt fraction, that are more important for irrigation agriculture [13]; [7].

The ECe of the saturation paste rarely exceeded 4 dS/m at 25 °C which indicates a very low hazard of salinity in these soils? The types of salts, as given from analysis of the exchangeable and soluble cations and anions, are dominantly sulphates followed by chlorides. Bicarbonate is present in little amounts while carbonates are either as a trace or not detected. The exchange complex in soils of this area is fully saturated with basic cations of Ca++, Mg++, Na+, and K+. Exchangeable H+ and Al+++ (exchange acidity) is therefore, non-existing.

The Cation Exchange Capacity CEC ranges from 40 – 70 meq/100gr soil. Exchangeable Potassium and sodium are determined separately and results indicated that potassium, whilst adequate for agricultural purposes, is very low compared to sodium. The Ca++ + Mg++ are calculated by difference between the CEC and exchangeable Na+ + K+, and therefore are not reported separately. This approach is adopted because of the occurrence of calcium sulphate in water adding more Ca++ and Mg++ to the soil solution which likely giving rise to erroneous estimates. The Sodium Adsorption Ratio (SAR) values are used to assess if there is any adverse effect of sodium in waters and soils.

4 ENTISOLS

4.1 Surface Features and Morphological Properties

Most of the soils of the Entisol order belong to the suborder Fluvents (from the Latin fluvius, river). These are brownish to reddish Entisols. They have formed in recent water-deposited sediments---primarily flood plains, fans, and deltas of rivers and small streams, but not in back swamps where drainage is poor (Figure 7). The age of sediments in which these soils form is usually very young, only a few years or decades. Under normal conditions Fluvents are flooded frequently, and deposited materials show signs of stratification---layers of a given texture alternated with layers of other textures. Most alluvial sediments, coming from eroding surfaces or stream banks, include very few amounts of organic carbon that are dominantly associated with the clay fraction. These soils do not occur under any specific vegetation type and may be found in most moisture or thermal regimes

Figure 7: Entisols Profile (Typic Torrifluvents) at study area

4.2 Physical properties

The Entisols soils are relic high-level abandoned meanders and oxbows flanking both sides of Atbara River. The characteristic reddish recent alluvium soils developed in-situ from alluvial parent materials derived from Basement and sandstone formations, and also Tertiary volcanic rocks in the Atbara River catchment within Ethiopia. These rocks are rich in Ferro-magnesium minerals. The recent and semi-recent soils appear to be much younger than the surrounding deposits and they are remnants of an alluvial landscape formation, probably during the Pleistocene and exposed to intensive alternating wet and dry periods [26]. The soils are very limited in extent and occupy relatively convex sites. Locally they are termed “Lebad”. They are characterized by their brownish colour, silty clay textures, moderate CEC, relatively high permeability and moderate nutrient status. Soil management difficulties on these soils might result largely from sealed surfaces, hard consistence of the surface horizons, relatively high concentrations of salts and the relatively low natural fertility status.

4.2.1 Soil depth and Bulk density

The depth of the non-Aridisols (recent and semi-recent deposits) is generally very deep at both southern and northern Parts of the area. No substratum rock materials were encountered at the alluvium soils sites. The bulk density of Entisols and Aridisols was not measured by the laboratory. However, data from geotechnical tests from the main canals at Study area indicated that the bulk density ranges from 1.3 – 1.7 g/cc (oven dry moisture) and 1.4 – 1.8 g/cc (at 1/3 bar moisture

4.2.2 Soil structure and texture

The surface is slightly hard dry, friable moist, sticky and plastic wet. It has a strong fine; medium and coarse sub-angular blocky structure. The subsoil is characterized by hard dry, friable moist, sticky and plastic wet consistence. The structure is dominantly weak, fine and medium sub-angular blocky. There is some surface cracking (cracks and tiny fissures 1-3mm) are observed but often the topsoil has a firm compacted surface with a sandy smear. The sandy clay loam surface and sandy clay subsoil and substratum have few to common CaCO3 and Fe-Mn concretions (0.5 – 2 cm) but as well clayey textures were noticed at some topsoil horizons. The soils are relatively high in sand content and there is less silt when compared with the Aridisols. The lower clay content results in a lower CEC than in the Aridisols although the mixed mineralogy typical of the alluvial sediments will contain the usual kaolinite and montmorillonite plus the iron oxide mineral goethite [4].

4.2.3 Soil drainage and drainability

Saturated hydraulic conductivity tests to indicate soil drainability were only conducted on Aridisols because it is known that wet Aridisols are essentially impermeable. Tests were carried out in-situ on the inferred least permeable horizon within 2.0 m, by the inverse auger method. Table 3 summarises the hydraulic conductivity results.

Table 3:Saturated Hydraulic Conductivity of Entisols

Profile number	Soil unit	Soil texture	Average K m/day
			1
80	A	Clay loam	1.09
352	G	Clay loam	1.50

Hydraulic conductivity results are regarded as indicative rather than precise. As regards interpretation, values below 0.2 m/day indicate slow – practically un-drainable soil and values up to 0.5 m/day suggest that either drainage may be required or irrigation should be applied in amounts and frequency consistent with a slow to moderate permeability, to avoid ponding. The substratum silt loam layers dominated by silt (silt about 50% of the particle sizes) could be the cause of the slow permeability of these soils. Although the control section of the Entisols soil is often dominated by coarse and fine loamy texture, it is normally separated by fine and coarse silty layers with more than 65% silt (Figure 7) that largely affect water movement and hence infiltration rate is controlled by these layers. Silty layers with fine and medium prismatic, angular and sub-angular blocky have an estimated hydraulic conductivity between 0.1 – 0.5 m day^{-1}. The field results fairly lie within this range indicating that the hydraulic conductivity is mainly controlled by these layers.

4.2.4 Infiltration

The infiltration rates should be interpreted as indicative rather than definitive and can vary considerably. Lack of a good correlation between infiltration and soil texture suggests that infiltration is more affected by soil structure, porosity, cracking or disturbance. Table 4 shows the infiltration test

results for Entisols in Study area. Infiltration rates of between 0.5 and 2.0 cm/hr. are considered optimum for gravity irrigation. Rates up to 6.0 cm/hr. are increasingly marginal for successful gravity irrigation and rates beyond 6.0 cm/hr. are so high that very small basins or short furrows are required. Sprinkler irrigation is not restricted by high infiltration rates. Results show that the increasing clay content of the subsoil affected the slow (0.2 – 0.5 m/day) hydraulic conductivities of these soils, whereas the sandy topsoil enhanced their moderate (2.0 – 6.0 cm/hr.) infiltration rate.

Table 4: Infiltration Rate of Entisols

Profile number	Soil unit	Soil texture	Replicate cm/day		
			1	2	3
296	A	Clay loam	3.0	2.0	2.7
374	G	Clay loam	3.2	3.2	3.6

4.3 Available Water Capacity

The available water capacities according to the soil units are shown in Table 13. Given that in semi-arid zones where there is little accumulation of organic matter and where soil structures tend to be weakly developed, AWC is primarily related to soil texture [27]. This varies considerably within and between soils, so there is a corresponding variability of AWC as evidenced by the disparity between minimum and maximum values per soil unit. AWCs, calculated from the soil texture, range from 135 mm to 153 mm for the top 1.0 m of soil. The overall average is 148 mm/m [3]. Based on all the study data arranged per soil unit the following classification of AWC can be derived (Table 5). Soil units A and B (Atbara and Gash) have not been further separated according to their topsoil texture because the effect of sandy or loamy topsoil does not consistently affect the soil AWC; there is more variation due to other un-quantified factors (subsoil textures, structure, consistence, organic content, clay minerals assemblage). For irrigation design purposes groups of soil units can probably be characterised by the average of their AWC class, but with the proviso that at implementation the irrigation frequencies and applications may vary significantly about this average. Average minimum values are 55% to 65% of average values for the moderate AWC, low AWC and very low AWC classes.

Table 5:Classification of AWC (mm/m) of Entisols at Study area

AWC class	Average	Range of average values	Range of minimum values	Average minimum value	Soil units A and G
Moderate	170	160 – 180	150 – 170	160	**A**Atbara old alluvium -pit 335 G Gash old alluvium -pit 194

It is to be remembered that not all of the soil AWC is readily available to plants. Readily available water content was not measured but a rule-of-thumb is that it is about half to two-thirds of total AWC [10]; [27]

4.3.1 Soil Taxonomic Classes of Aridisols And Entisols

The soil types have been classified according to the Soil Taxonomy [16[. This classification is based on the soils' control section (usually the 0.25 m – 1.00 m depth) and is shown in Table 6. The typical classification is given and also the classification of the soil phase where different from the classification of its soil unit. For example, a sodic phase of soil unit G will be classified differently from the typical G.

The soil properties that have been considered during the soil study to classify the soil units and their phases are: Topsoil and subsoil texture classes; Evidence of recent alluvial deposition; Degree of soil profile development; Presence, quantity and distribution of CaCO3; Levels and distribution of SAR; Levels and distribution of EC and Presence, nature and distribution of gypsum content.

Table 6: TheIdentified Taxonomic Classes in the Study Area

Soil unit class	**Code**	**No. in class**
Vertic Haplocambids	VHC	194
Typic Torrifluvents	TTF	65
Typic Haplocambids	THC	52
Fluventic Haplocambids	FHC	33
Vertic Torrifluvents	VTF	23
Typic Torripsamments	TTS	7
Typic Haplocalcids	THD	6
Number of classes in all pits		**380**

REFERENCES

[1] Blokhuis, W.A., L.H.J. Ochtman, and K.H. Peters. 1968. Aridisols in the Gezira and Khashm el Girba clay plains, Sudan. Trans 8th Intern. Congress Soil Science, Bucharest Romania. VolV: 591-603.

[2] Blokhuis, W.A. 1993. Vertisols in the Central Clay Plain of the Sudan. PhD Thesis, Agricultural University Wageningen. 418 pages.Wageningen.

[3] Brady N. C. 1974. The Nature and Properties of Soils. 8th edition. Macmillan publishing Co. Inc. New York.

[4] Buursink, J.,1971. Soils of Central Sudan.PhD Thesis, Utrecht University. 248 p. Utrecht.

[5] DIU. 2014. Semi Detailed Soil Survey of Upper Atbara Irrigation Project Area. Volume 1: Main Report (Final Report). Dams Implementation Unit,Khartoum. Sudan

[6] FAO, 1970. Soil Survey of the Gash and Tokar Deltas. AGL:SF/SUD 15. Technical Report No. 4. Rome. Italy

[7] FAO, 1995.Integrated Plant Nutrition Systems. FAO Fertilizers and Plant Nutrition Bulletin – No.12

[8] FAO, 2006. Guidelines for Soil Description.4th edition. Rome

[9] Lahmeyer International. 2008. Development Options – Upper Atbara Irrigation Project, Technical Note 04 - 280212-3.doc. Dams Implementation Unit (DIU), Khartoum.

[10] Grossman et al., 1985. Application of pedology to plant response prediction For tropical Vertisols Proceeding of the Fifth international Soil classification workshop. Soil study Administration, Khartoum. Sudan

[11] Landon, R. (editor), 1991. Booker Tropical Soil Manual - A handbook for soil survey and agricultural land evaluation in the tropics and subtropics Paperback Edition, Longman Scientific Technical Co-published in USA with John Wiley & Sons. Inc. New York

[13] Masdar, 1994. South Kassala Agricultural Development Project (SKAP).Ministry of Agriculture, Khartoum.

[14] Mohamed, A. S. 1992/93. Effect of Phosphorus, Zn and Cu on wheat yield and nutrients content.Annual Report.GRS. Wad Medani, Sudan

[15] Newtech / HTSPE, 2009.Study of the Sustainable Development of Semi-Mechanized Rain-Fed Farming. Ministry of Agriculture, Khartoum

[16] Obeid, M. and Seif El Din.A., 1970. Ecological studies of the vegetation of the Sudan. Acacia senegal (L) wild and its natural regeneration, J. App.. Ecol. 7:502-518.

[17] Soil Survey staff. 2014. Keys to Soil Taxonomy, 12th edition. United States Department of Agriculture, (USDA). Washington,DC.

[18] Sogreah, 2007.Upper Atbara Irrigation Project. Project Review

[19] Sombroek, W. G. 1971. Aridisols of the World, Occurrence and Potential.Fourth International Soil Correlation Meeting (ISCOM), Lubbock, TX USA.Working Paper and Preprint No. 87/2. International Soil Reference and Information Centre (ISRIC). Wageningen, The Netherlands.

[20] SSA, 1973.Reconnaissance Soil Survey in the Upper Atbara Area.Hussam el Sayed Farah. SSA Report 48. Wad Medani.

[21] SSA, 1976. Exploratory Soil Survey of Kassala Province. A study of the physiography, soils, and agricultural potential.V. Van der Kevie and Ibrahim Buraymah.SSA Report, No. 73. Wad Medani.

[22] SSA, 1980. Semi-detailed soil survey and land suitability classification of Sitit area. Ahmed Abdel Raouf Khalil. SSA Report, No. 106. Wad Medani.

[23] SSA. 1983. Semi-detailed soil survey report of the Gash-Kassala Area. Abd el MoniemMohed Ahmed Kafeel. SSA Report, No. 123. Wad Medani.

[24] Swan, C.H. 1961. The Recorded Behaviour of the River Gash in the Sudan.Ministry of Irrigation and Hydro-electric Power, Khartoum.

[25] Van der Kevie, W. (Editor). 1976. Manual of land Suitability Classification for Agriculture, SSA, Wad Medani, Sudan.

[26] Whiteman, A.J., 1971. The Geology of the Sudan Republic, Oxford University Press,

[27] Williams, M.A.J. and Adamson, D.A. (eds.), 1982. A land between two Niles Quaternary geology and biology of the Central Sudan. Rotterdam: Bolkema

[28] Saxton, K. E., Rawls, W. J. 2006. Soil Water Characteristic Estimates by Texture and Organic Matter for Hydrologic Solutions. Soil Sci. Soc. Am. J. 70:1569–1578 (2006). Soil Science Society of America 677 S. Segoe Rd., Madison, WI 53711 USA

ACKNOWLEDGEMENTS:

The authors would like to acknowledge with great appreciation the effort extended by the supporting soil field and laboratory staff from College of Agricultural studies, LWRC lab team and by the soil field staff from Khartoum state Ministry of Agriculture. The supervision support provided by senior colleagues; Abdulkaareem O Fadl, Hashim Ali Dawoud, Fawzi M. Salih and Hussain Abu Zaid is highly appreciated.